MODELING THE POLARIMETRIC RESPONSE OF ICE AND REGOLITH IN BISTATIC RADAR OBSERVATIONS OF THE LUNAR POLES. P. Prem[1a], G. W. Patterson[1], A. K. Virkki[2], S. S. Bhiravarasu[3,4], D. T. Blewett[1], J. T. Cahill[1], [1]Johns Hopkins Applied Physics Laboratory, 11100 Johns Hopkins Rd., Laurel, MD, US; [2]Arecibo Observatory, University of Central Florida, Arecibo, PR, US; [3]Lunar and Planetary Institute, USRA, Houston, TX, US; [4]ISRO Space Applications Centre, Ahmedabad, India; [a]parvathy.prem@jhuapl.edu.

Introduction: Ground-based and orbital radar observations of the Moon have played a significant role in the search for water ice at the lunar poles (e.g., [1-2], and references therein). Remote sensing at radar wavelengths has the twin advantages of being able to see beneath the lunar surface, and to respond to the physical form of water ice, if it is present in sufficient quantity.

The Mini-RF instrument onboard the Lunar Reconnaissance Orbiter is currently operating in a bistatic mode, in which the instrument acts as a receiver for signals transmitted at S-band (12.6 cm) from the Arecibo Observatory and at X-band (4.2 cm) from the DSS-13 antenna at the Goldstone Deep Space Communications Complex. These observations allow for the construction of a unique view of the lunar surface, in which the polarimetric characteristics of various terrains can be examined at a range of incidence and bistatic (phase) angles. Bistatic observations allow for the characterization of a response referred to as the Coherent Backscatter Opposition Effect (CBOE), caused by multiple scattering within a medium, and associated with increases in the intensity of backscattered radiation and the Circular Polarization Ratio (CPR) at small phase angles [3].

The icy moons of Jupiter and Mercury's polar water ice deposits all show high radar CPR at zero phase, consistent with CBOE [4, 5]. However, radar observations of the lunar poles tell a story that is less clear-cut, for several reasons: (i) multiple studies concur that there is an absence of thick, pure deposits of ice within the upper few meters of the subsurface, however the response of ice-regolith mixtures at radar wavelengths is not definitively known; (ii) observations of the lunar poles have often been made at very oblique angles of incidence (> 80°), which can alter the radar response in ways that are not yet comprehensively understood. In this context, our present work aims to address the following questions: (i) How do polarimetric properties (e.g., CPR) vary as a function of bistatic angle for ice and regolith analogs at radar wavelengths, at varying angles of incidence? (ii) What constraints does this provide as to the abundance and physical form of water at the lunar poles?

Numerical Methods: We use an electric field Monte Carlo [6] code to model CBOE at varying incidence angles. This approach is based on tracking the propagation of a large number of "energy bundles" through the medium of interest. Each energy bundle is described by a Jones vector, which defines the polarization characteristics of the electromagnetic radiation represented by the bundle. The two components of the Jones vector are complex electric fields in two orthogonal directions, defined relative to the direction of propagation. Each scattering event modifies the Jones vector; the post-scattering vector is obtained by multiplying the pre-scattering vector by a scattering matrix, the terms of which depend on the properties of the medium at the wavelength of interest. We also account for attenuation of radiation along the propagation path. CBOE arises when time-reversed paths (traveling between the same set of scattering points in opposite directions) interfere. In an electric field Monte Carlo implementation, interference can be computed by adding the corresponding electric field vectors. Figure 1 is a schematic depiction of this approach.

For circularly polarized incident radiation, CPR is defined as the ratio of the same-circular (SC) and opposite-circular (OC) components of the received signal.

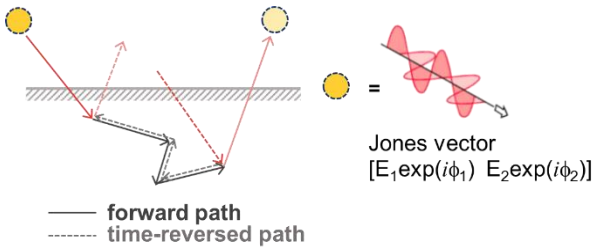

Figure 1. *Schematic view of the electric field Monte Carlo approach used in this work.*

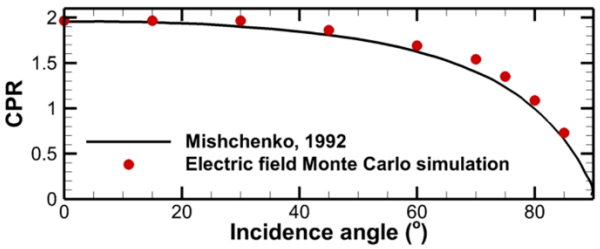

Figure 2. *Results obtained using the electric field Monte Carlo approach, and an analytical solution for spherical particles with refractive index 1.45 and effective radius equal to the wavelength of incident radiation [7].*

Results: In order to validate the modeling approach described above, we simulated a previously studied sce-

nario [7] and found good agreement between our numerical results and an analytical solution. This result is shown in Figure 2 to emphasize that in these simulations, CPR generally decreases with increasing incidence angle, contrary to the increase in CPR with incidence angle typically observed in radar datasets [8]. This is due to the fact that we do not currently account for the specular component that dominates OC radar return at small incidence angles. Since we are particularly interested in large (> 80°) angles of incidence, at which the volume-scattering component dominates [9], we presently focus on only the volume-scattered component. Figure 2 also shows that at higher angles of incidence, CPR is more sensitive to changes in incidence angle, suggesting that it may be particularly important to account for the effects of local slopes when conducting bistatic observations of polar targets.

We then investigated the response of four simulated media, shown schematically in Figure 3a. We approximate the scattering and attenuation properties of (i) blocks of ice, (ii) blocks of rock, (iii) spherical "clumps" of fine-grained regolith, and (iv) ice with internal voids (vacuum), by considering the interaction of representative spherical volumes (i.e. Mie scattering), 2 cm in diameter, with 12.6 cm (Arecibo S-band) radiation. Complex refractive indices of ice, rock and regolith are derived from the dielectric constants used in previous modeling work [9], with an arbitrary volume filling factor of 0.433. Although Mie theory is derived for isolated spherical scatterers (unlikely to be the case in a planetary regolith), this is an interesting approximation to start with, and one that has been previously adopted to investigate coherent backscatter [5].

Figures 3b and 3c show CPR as a function of phase angle for incidence angles of 0° and 80°, respectively. In all four cases, we see a broadening of the opposition response and an overall decrease in CPR at oblique incidence. This decrease in CPR is attributable to a decrease in the amount of multiply scattered radiation (which tends to preserve the sense of polarization) that reaches the receiver at oblique angles of incidence. We also find that in the monostatic case (zero phase), CPR is highest for voids in ice, followed by blocks of ice, blocks of rock, and then regolith. This decrease follows from increasing attenuation (decreasing single-scattering albedo) of radiation in these media. Quantitatively, we note that the 80° simulations result in significantly lower values of CPR, and a more subdued rise towards zero phase than are seen in bistatic observations at similar angles of incidence [2]. This is likely due to differences in the scattering properties of actual lunar terrains compared to idealized media.

These initial results indicate that in order to quantitatively interpret bistatic data acquired over a range of incidence angles, it is important to characterize (i) the scattering properties of the lunar surface at radar wavelengths, and (ii) the sensitivity of CBOE to incidence angle. We aim to pursue these questions by leveraging recent, more detailed investigations into the scattering properties of particulate media [10], particularly mixtures of ice and regolith, and by exploring incidence angle space more fully. We will report on our progress towards these objectives, and discuss implications for understanding subsurface composition and structure at the lunar poles.

Acknowledgments: This work was supported by NASA's Lunar Reconnaissance Orbiter mission through funding to the Mini-RF instrument team.

References: [1] Nozette et al. (1996), *Science* 274, 1495-1498; [2] Patterson et al. (2017), *Icarus* 283, 2-19; [3] Hapke (1990), *Icarus* 88, 407-417; [4] Slade et al. (1992), *Science* 258, 635-640; [5] Black et al. (2001), *Icarus* 151, 167-180; [6] Sawicki et al. (2008), *Optics Express* 16, 5728-5738; [7] Mishchenko (1992), *Earth, Moon & Planets* 58, 127-144; [8] Carter et al. (2011), *Proc. IEEE* 99, 770-782. [9] Fa et al. (2011), *JGR* 116, E03005; [10] Virkki & Bhiravarasu (2019), *JGR* 124, 3025-3040.

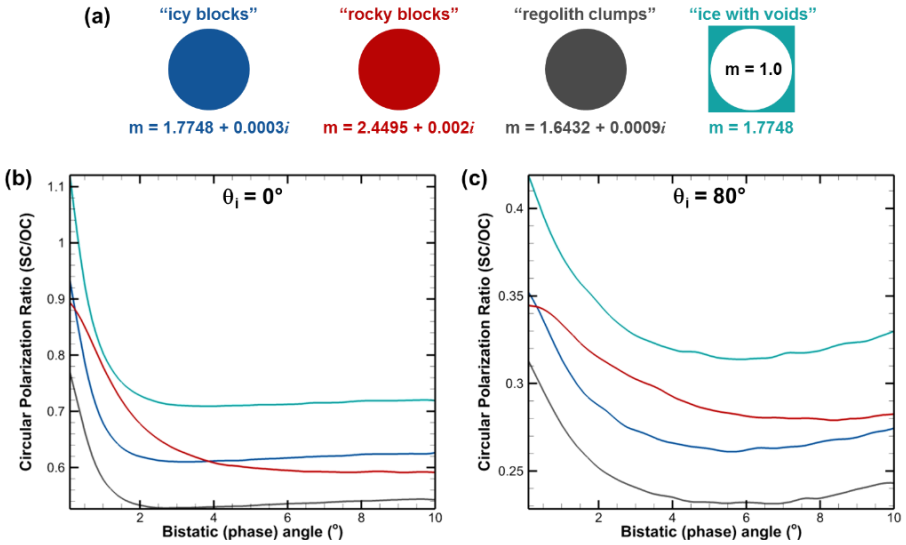

Figure 3. *(a) Schematic view of the four different media simulated, and their complex refractive indices. (b) CPR vs. bistatic angle at 0° and (c) 80° incidence. Note that y-axis scales are different.*